RSC Advances

ROYAL SOCIETY OF CHEMISTRY

www.rsc.org/advances

Synthesis and self-assembly of well-defined binary graft copolymer and its use in superhydrophobic cotton fabrics preparation

Yinwen Li [a, b, c,*], Xiuwen Zheng [a], Huayu Zhu [a], Kun Wu [b], Mangeng Lu [b]

a School of Chemistry & Chemical Engineering, Linyi University, Linyi 276000, PR China.

b Key Laboratory of Cellulose and Lignocellulosics Chemistry, Chinese Academy of Sciences, Guangzhou institute of Chemistry, Chinese Academy of Sciences, Guangzhou 510650, PR China.

c University of Chinese Academy of Sciences, Beijing 100039, PR China.

Abstract

We have synthesized and characterized series of functional binary graft copolymers PGMA-g-(PHFBMA-r-POEGMA)s(BGCs). First, PHFBMA-C≡CH, POEGMA-C≡CH and P(GMA-N_3) were synthesized via sequential atom transfer radical polymerization (ATRP). BGCs were prepared by grafting of alkyne-end poly (hexafluorobutyl methacrylate) (PHFBMA-C≡CH) and poly (oligo (ethylene glycol) methyl ether methacrylate) (POEGMA-C≡CH) onto poly (3-azide-2-hydroxypropyl methacrylate) (P(GMA-N_3)) via click chemistry. The self-assembly behaviors were investigated by combination of dynamic light scattering (DLS), transmission electron microscopy (TEM), and atomic force microscopy (AFM). Since POEGMA was soluble in water while PHFBMA was insoluble, BGCs self-assembled and produced stable PHFBMA-centered nano-micelles; Then BGCs were used to fabricate hydrophobic cotton fabrics. While the PHFBMA block provided low surface free energy, the POEGMA block served as an anchor with cotton fibers, the modified cotton fabrics showed excellent superhydrophobic property. The results confirmed that fluorinated surface was formed onto substrate without changing the transparency and bulk composition of the cotton fabrics. Moreover, SEM and AFM analysis indicated that nano- and microscale roughness

were created by combining BGC-based nano bumps onto surfaces of micro-sized cotton fabrics.

Keywords: Binary graft copolymers; Amphiphilic fluorocopolymer; Self-assembly; Superhydrophobic

Introduction

Synthesis and self-assembly of amphiphilic linear block copolymers with well-defined compositions and structures have been one of the most important research topics in polymer science over the past few decades, and numerous well-designed amphiphilic polymers have been developed and widely adopted for academic and applied polymer science.[1-6] However, amphiphilic block copolymers bearing more complex segments such as multiblock, star, comb-like, dendrimers, etc. are not as actively reported partly due to their relatively challenging synthesis and characterization.[7-10] Among them, amphiphilic graft copolymers consist of macromolecules in which one or several grafts are attached to the main polymer backbone as side chains, and the grafts and backbone derive from different monomers. When two or more different side chains are attached to a polymer backbone, binary, ternary, and multi-graft copolymers will be formed, and each side chain behaves like a block segment. The spatial arrangement of different side chains along the backbone and their relative ratio dramatically affect their self-assembly behaviors.[11-15] Because of the mutual incompatibility of different side chains, the constituent side chains of graft copolymer usually undergo microphase separation in bulk and in concentrated solution. This phenomenon is important especially in selective solvents, and can result in the formation of stable micelles; therefore, controlled synthesis of these graft-like copolymers would significantly expand the library of polymeric materials and make it possible to explore their physicochemical properties for potential applications.

Many naturally occurring surfaces behave non-wetting abilities in order to fulfill their functional demands, and great interests have been inspired for scientists and engineers to develop similar artificial superhydrophobic surfaces with a variety of functionalities.[16-22] A superhydrophobic surface is defined as a surface on which has contact angle (CA) of more than 150^{o} and sliding angle (SA) of less than 10^{o}. These properties are attractive for many industrial and biological applications such as self-cleaning paints, coatings for windows, textiles and solar panels, anti-icing, anti-fogging, protection of electronic devices etc.[23-31]

It has already found that superhydrophobic surfaces in nature possess nano- and microscale roughness and low free surface energies.[32-36] Inspired by these findings, artificial superhydrophobic surfaces are fabricated by creating hierarchical micro- and nano-structures on hydrophobic substrates, or modifying hierarchical structured surfaces with low surface free energy materials. Moreover, many approaches for mimicking natural superhydrophobic surfaces have been developed over the past decades, such as sol-gel chemistry, co-condensation, layer-by-layer deposition, hydrothermal synthesis, electrospinning, chemical deposition and lithographic methods. [37-45]

The chemical modification with low surface energy functionalities, especially fluorine containing hydrocarbons or perfluorosilanes, is an efficient and practical method to fabricate hydrophobic surfaces.[46-51] Small fluorinated molecules for preparing coatings and fluorinated silica nanoparticles have been widely used to produce rough superhydrophobic surfaces. However, in many cases the deposited layer on the surface has a thickness equal to or higher than the particle diameter, and such a thick coating layer might change the intrinsic properties of the substrates and damage its transparency. Moreover, in view of its cost and poor water solubility, fluorinated compounds or polymers always involve large amounts of organic solvents which could cause negative effects on environment, and are highly unlikely to be employed in commercial applications.[52-57] Thus, the typical way to prepare a fluorinated

surface is to graft a thin layer of a fluorinated water soluble compound onto the substrates without changing the bulk composition of the substrates.

To meet the challenges associated with developing cotton fabrics with improved superhydrophobic surfaces, we designed and prepared a novel functional binary graft copolymer, PGMA-g-(PHFBMA-r-POEGMA) (BGC), which is shown in Scheme 1. The graft-onto method was used to produce the desired binary graft copolymer. The backbone polymers used were two poly (3-azido-2-hydroxypropyl methacrylate), P(GMA-N_3)s. The grafts used were water insoluble alkyne-end poly (hexafluorobutyl methacrylate) (PHFBMA-C≡CH) and water soluble poly (oligo (ethylene glycol) methyl ether methacrylate) (POEGMA-C≡CH), respectively. The precursory grafts PHFBMA-C≡CH and POEGMA-C≡CH were coupled to P(GMA-N_3) via Cu catalyzed alkyne-azide cycloaddition. According to our experiment, the (-C≡CH) to (N_3) molar ratio was determined to 30/100-40/100, and the residual N_3 groups were then deactivated by reaction with propargyl alcohol. The results showed that the cotton fabrics coated with BGCs exhibited excellent superhydrophobic property, and the method demonstrated in this paper might has potential application prospect for the superhydrophobic surfaces fabrication.

2 Experimental

Materials

Propargyl alcohol, 2-methoxyethanol, 2-bromoisobutyryl bromide (BIBB), and 2, 2, 3, 4, 4, 4-hexafluorobutyl methacrylate (HFBMA) were all purchased from Aladdin Reagent Co. Ltd., China. 2-(2-methoxyethoxy) ethyl methacrylate (MEO_2MA, Mn=188.2 $g \cdot mol^{-1}$) was acquired from TCI, Japan, and passed through short basic alumina column in order to remove inhibitor before use. Glycidyl methacrylate (GMA) (Aladdin Reagent Co. Ltd., China) was purified by passage through acolumn of alumina powder to remove the inhibitor before use. Cuprous bromide (CuBr, Aladdin Reagent Co. Ltd., China) was stirred in acetic acid at 80 ^oC for 8 h,

washed three times with methanol, and dried under vacuum overnight at room temperature. Triethylamine (TEA, Aladdin Reagent Co. Ltd., China) were stirred with CaH_2 overnight before distillation. Sodium azide, (N, N, N, N, N-pentamethyldiethylenetriamine (PMDETA, 99%) and 2, 2-bipyridine (bpy) (99%) were all purchased from Aladdin Reagent Co. Ltd., China. Cyclohexanone, diphenyl ether, DMF, THF, CH_2Cl_2, diethyl ether, and hexane were all analytical grade and used as received.

Synthesis of 2-alkyne 2-bromoisobutyrate (ABIB)

Alkynyl-end ATRP initiator ABIB was synthesized by the reaction of propargyl alcohol and 2-bromoisobutyl bromide using triethylamine as acid acceptor in anhydrous tetrahydrofuran. A typical procedure is described as follows: to a stirred solution of propargyl alcohol (5.6 g) and triethylamine (15.2 g) in 150 mL of anhydrous tetrahydrofuran at 0 ºC, 2-bromopropionyl bromide (57.5 g) was added dropwise for 2 h. The reaction was kept for another 2 h at 0 ºC and then left for 40 h at room temperature. The precipitate was filtered out and the filtrate was washed in sequence with 0.1 N HCl, saturated sodium carbonate, and distilled water for three times before dried over anhydrous magnesium sulfate for at least 12 h. The crude product was isolated as a slight yellow liquid after removed of the solvent and then concentrated by rotary evaporator. The concentrated liquid purified by silica gel column chromatography using ethyl acetate/petroleum ether (1:5 v/v) as the eluent. After removed the solvents by a rotary evaporator and dried in vacuum oven at 40 ^oC for 24 h. ABIB was obtained as slight yellow liquid, Yield: ≈ 77%. ^{1}H-NMR (400 MHz, $CDCl_3$, δ): 4.77(2H, CHCCH_2-), 2.51(1H, -CCH), 1.95(6H, -CH(CH_3)$_2$Br).

Synthesis of PHFBMA-C≡CH

PHFBMA-C≡CH was synthesized by the ATRP of HFBMA monomer using ABIB as the ATRP initiator. A typical procedure is described as follows: the schlenk tube was purged with dry argon for 30 minutes, a degassed mixture of HFBMA (2.5 g), cyclohexanone (10 g),

ABIB (0.11g) initiator and copper bromide (0.058 g) was added to a schlenk tube, degassed via three freeze-thaw-pump cycles and back-filled with argon. Then 2, 2- bipyridyl (0.13 g) were added. The mixture was heated at 60 °C in an oil bath for 4 h. The experiment was stopped by immersing the tube into liquid nitrogen and then exposing the contents to air. The final mixture was diluted in CH_2Cl_2 and passed through a short neutral alumina column in order to remove copper catalyst. Then the filtrate was subsequently added into 500 mL of hexane to precipitate, and the precipitate was dried under vacuum for 24 h to get white powder, Yield: ≈ 89%. ^{1}H NMR (400 MHz, $CDCl_3$, δ): 4.86-4.96 (H, -C*H*F-), 4.71-4.73 (2H, CHC-C*H*$_2$-O-), 4.33-4.36 (2H, -OC*H*$_2$-CF_2-), 2.30-2.31 (H, C*H*C-), 1.8-2.0 (2H,-C*H*$_2$-), 0.86-1.45 (3H, -C*H*$_3$).

Synthesis of POEGMA-C≡CH

POEGMA-C≡CH was synthesized by the ATRP of MEO_2MA monomer using ABIB as the ATRP initiator. A typical procedure is described as follows: the schlenk tube was purged with dry argon for 30 minutes, a degassed mixture of MEO_2MA (3.76 g), cyclohexanone (10 g), ABIB (0.11g) initiator and copper bromide (0.058 g) was added to a schlenk tube, degassed via three freeze-thaw-pump cycles and back-filled with argon. Then 2, 2- bipyridyl (0.13 g) were added. The mixture was heated at 60 °C in an oil bath for 4 h. The experiment was stopped by immersing the tube into liquid nitrogen and then exposing the contents to air. The final mixture was diluted in CH_2Cl_2 and passed through a short neutral alumina column in order to remove copper catalyst. Then the filtrate was subsequently added into 500 mL of hexane to precipitate the polymer, and the precipitated viscous solid was dried under vacuum for 12 h, Yield: ≈82%. ^{1}H NMR (400 MHz, $CDCl_3$, δ): 4.71-4.73 (CHC-C*H*$_2$-O-), 3.34 (C*H*$_3$-O-), 3.44-4.05 (-C*H*$_2$-C*H*$_2$-O-), 2.30-2.31 (C*H*C-), 1.8-1.85 (2H,-C*H*$_2$-), 0.86-1.45 (-C*H*$_3$).

Synthesis of 2-methoxyethyl 2-bromoisobutyrate (MBIB)

MBIB was prepared by reaction between 2-methoxyethanol and 2-bromoisobutyryl bromide in dry diethyl ether at room temperature and the typical procedure is described as follows: to a round-bottomed flask charged with 200 mL of anhydrous diethyl ether, ethylene glycol monomethyl ether (3.04 g) and triethylamine (6.07 g) was added, the solution was cooled down to about 0 ºC, 2-bromobutyryl bromide (18.4g) was added in drops for 2 h. The reaction was proceeded for another 2 h at 0 ºC and then left for 48 h at room temperature. The precipitate was filtered out and the filtrate was washed in sequence with 0.1 N HCl, saturated sodium carbonate, and distilled water for three times before dried over anhydrous magnesium sulfate. The crude product was isolated as a slight yellow liquid after removed of the solvent and then concentrated by rotary evaporator. The concentrated liquid purified by silica gel column chromatography using ethyl acetate/petroleum ether (1:4 v/v) as the eluent. After removed the solvents by a rotary evaporator and dried in vacuum oven at 40 ^{o}C for 24 h. MBIB was obtained as a slight yellow liquid, yield ≈ 72 %. ^{1}H NMR ($CDCl_3$): δ (ppm) 4.31-4.34 (2H, -C*H*$_2$COO-), 3.63-3.65 (2H, CH_3OCH_2-), 3.40 (3H, C*H*$_3$O-), 1.95 (6H, -C(C*H*$_3$)$_2$).

Synthesis of PGMA

$PGMA_{50}$, and $PGMA_{100}$ were prepared via ATRP by using MBIB as the initiator and CuBr/PMDETA as the catalyst system. A typical procedure for $PGMA_{50}$ is described as follows: the schlenk tube was purged with dry argon for 30 minutes, then degassed diphenyl ether (5.0 mL), MBIB (0.1 g), GMA (2.4 g) CuBr (0.0485 g) were added to the schlenk tube, degassed via three freeze-thaw-pump cycles and back-filled with argon. Then degassed PMDETA (0.1172 g) was injected into the flask using a degassed syringe, and the tube was then immersed in a preheated oil bath at 28 °C for 15 min for GMA polymerization. The experiment was stopped by immersing the tube into liquid nitrogen and then exposing the contents to air. The resultant viscous reaction mixture was diluted with CH_2Cl_2 (50 mL) and passed through a short neutral alumina column in order to remove copper catalyst. The

filtrate was subsequently added into 500 mL of hexane to precipitate the polymer. It was redissolved in 40 mL of CH_2Cl_2 and precipitated into 500 mL of hexane again. The precipitate was dried under vacuum for 12 h, yield≈ 98 %. ^{1}H-NMR (400 MHz, $CDCl_3$, δ): 3.78, 4.29 (-COOC*H*$_2$-), 3.53~3.58 (CH_3OCH_2-), 3.34 (CH_3O-), 3.23 (-CH_2OC*H*-), 2.61, 2.82 (-C*H*$_2$OCH-), 1.74~2.04 (-C(CH_3)C*H*$_2$-), 0.79-1.14 (-C(*CH*$_3$)CH_2-). $PGMA_{100}$ were prepared analogously, except the use of different GMA to initiator molar ratios (110.5:1).

Synthesis of P(GMA-N_3)

To attach azide groups, PGMA was reacted with NaN_3. Taking $PGMA_{50}$ for example, a typical procedure is described as follows: $PGMA_{50}$ (0.72 g, 5.0 mmol of epoxide groups) was dissolved in DMF (50 mL). Sodium azide (1.63g) and ammonium chloride (1.34 g) was then added to polymeric DMF solution, which was subsequently stirred at 40°C for 48 h. After the reaction, insoluble impurities were removed by filtration. After most of the DMF had been evaporated, P(GMA-N_3)$_{50}$ was precipitated in excess amount water. The polymer was redissolved in~20 mL of DMF and precipitated into excess amount of water again. The product was filtrated, washed with water at least for three times, and vacuum-dried to give white solid, yield≈ 91%. ^{1}H-NMR (400 MHz, DMSO-*d6*, δ): 5.50 (-O*H*), 3.80~3.90 (-C*H*(CH_2N_3)OH, -COOC*H*$_2$-), 3.28 (-CH_2N_3), 1.33~2.06 (-C(CH_3)C*H*$_2$-), 0.57~0.98 (-C(C*H*$_3$)CH_2-).

Preparation of binary graft copolymers (BGCs)

In an example preparation, DMF (16.0 mL), P(GMA-N_3)$_{50}$ (0.086 g, 50 mmol of azide groups), PHFBMA-C≡CH (0.28 g), and an aqueous sodium ascorbate solution (0.1 mg, dissolved into 0.20 mL of water) were mixed in a 50 mL round-bottomed flask and deoxygenated via bubbling with argon for 50 min. Then, a saturated aqueous solution of $CuSO_4 \cdot 5H_2O$ (0.40 ml) was added. This was followed by stirring the reaction mixture at 50 ^{o}C for 24 h. Subsequently, 5.0 mL of a degassed DMF solution of POEGMA-C≡CH (0.80 g)

was introduced into the flask using a syringe. The reaction was allowed to go for another 48 h. lastly, degassed propargyl alcohol (0.80 g) was injected into the flask, and the reaction mixture was stirred for 24 h to deactivate the residual azide groups. The experiment was stopped by exposing the catalyst to air, then the final mixture was diluted with DMF and subsequently purified by dialysis in aqueous 5% EDTA solution (molecular weight cut off: 14000), finally purified by dialysis in aqueous solution for 48h, and freeze-dried in vacuum TGC was obtained as slight yellow solid, yield≈ 73%.

Micelles preparation

In a typical example, 10 mg of BGC_1 was dissolved in THF (1.0 mL) and stirred for at least for 24 h, and then under vigorous stirring, 10 ml deionized water was added slowly at a flow rate of 0.2 mL/min until the appearance of the solution with a characteristic bluish tinge. After the addition was completed, the dispersion was left stirring for another 24 h at room temperature, and THF was blown away by nitrogen. Aqueous solution with light bluish tinge was typically obtained; similar procedures were done to prepared micelles with different concentrations (1.0 mg/mL, 2.0 mg/mL, 4.0 mg/mL, 6.0 mg/mL, and 10.0 mg/mL).

Cotton fabrics modification with BGCs

In a typical procedure, five pieces of cotton fabrics (3.0 cm×2.5cm), 10 mL BGC aqueous solution were loaded into a 25 mL flask and stirred at room temperature for 30 min. The resulting cotton fabrics samples were first naturally dried at room temperature in desiccator for 2 d, then dried in an oven at 120 ^{o}C for 2 h. All of the cotton fabrics modified with BGCs described in this study were prepared similarly.

Characterization

FT-IR and ^{1}H NMR spectroscopy. FT-IR spectra were recorded on a Nicolet 5100 spectrometer by KBr sample holder method in the fundamental region of 400-4000 cm^{-1}. ^{1}H

NMR spectra were obtained on a Bruker DMX-400 spectrometer. Deuterated chloroform ($CDCl_3$), or deuterated dimethyl sulfoxide (DMSO-d_6) was used as the solvent.

Size exclusion chromatography (SEC). The number average molecular weights (Mn) and polydispersity index (Mw/Mn) values of the polymers were determined at 30 ^oC using a Waters 1515 size exclusion chromatography (SEC) system equipped with a Waters 2414 refractive index (RI) detector, and monodispersed PS was used as standards. DMF solution was used as eluent, and passed through a 0.45mm PTFE filter before analysis.

Dynamic light scattering (DLS). The hydrodynamic diameters (Dh) of the capsules and their polydispersity indices (PDI) were determined by dynamic light scattering (DLS) on a Malven Zetasizer Nano System (Nano-zs90). The solutions were passed through 0.45 μm filters before DLS measurements. The measurements were conducted in a 3.0 mL quartz cuvette, using the 670 nm diode laser, and the 90° scattering angle. Each set of Dh and PDI values was the average from five measurements.

Transmission electron microscopy (TEM). The morphology and architecture of nano-sized aggregates were visualized by transmission electron microscopy (TEM), and the samples were prepared by placing polymer aqueous solution on copper grids in a biochemical incubator thermostatted at 20 ^oC, and stained with phosphotungstic acid before observation on a JEM-100CX II microscope operated at 80 kV.

Scanning electron microscopy (SEM). The surface morphologies of cotton fabrics were characterized with a scanning electron microscope (SEM, Hitachi, S-4800) that was operated at an accelerating voltage of 2.0 kV. The samples were affixed onto an aluminum SEM-holder and coated with a thin layer of gold before observation.

Atomic force microscopy (AFM). The samples were fixed onto the surface of an AFM-holder, and the surface morphologies of the samples were observed using a Multimode 8 SPM AFM system (Bruker, USA) using the ScanAsyst TM mode.

X-Ray photoelectron spectroscopy (XPS). XPS measurements were performed using a surface science instruments X-ray Photoelectron Spectrometer/ESCA (ESCALAB 250, produced by Thermo Fisher Scientific), which was operated at a base pressure of $2\text{-}10^{-9}$ mbar.

Contact angle (CA) and sliding angle (SA) measurements. The CAs were obtained using a contact angle goniometer JC2000D1 (Power each Digital Technology Equipment Co., Ltd., Shanghai, China) by a drop-shape analysis method. The reported values were the average of 5 trials measured using 2 μL water droplets that were placed at different locations on the samples. SA was measured according to previous report.[52]

Resistance measurements. The chemical durability of the superhydrophobic cotton fabrics was evaluated by immersing the samples into aqueous solutions with different pH values and various organic solvents. After the samples had been immersed into the liquid for a predesigned time, the samples were dried in an oven at 60 ^{o}C for 24 h under vacuum before evaluation. The changes of the CAs and SAs as functions of the immersion time were recorded.

3 Results and discussion

Synthesis of monomers and binary graft copolymers

ABIB, MBIB, PGMA, P(GMA-N_3), PHFBMA-C≡CH, and POEGMA-C≡CH were first synthesized, and then the latter two polymers were grafted onto the P(GMA-N_3) backbone to yield PGMA-g-(PCEMA-r-POEGMA) copolymers. Scheme 2 shows the reactions used to prepare the individual monomers and final graft copolymers, BGCs.

PGMA and P(GMA-N_3). According to Scheme 2, PGMA was synthesized by ATRP following a modified literature method using diphenyl ether as the solvent, MBIB as the initiator, CuBr as the catalyst, and PMDETA as the ligand.[8.58, 59] Two PGMA homopolymers ($PGMA_{50}$ and $PGMA_{100}$ with GMA repeat units of 50 and 100) were synthesized using the monomer to initiator molar ratios $[M]_0/[I]_0$ of 50.4 and 110.5, respectively. The resultant

polymers were analyzed by FT-IR, ^{1}H NMR and SEC. Fig. 1 is the ^{1}H NMR spectrum for $PGMA_{50}$, as a matter of fact, the actual conversion ratio of this reaction was not up to 100%, the best mole ratio of MBIB to GMA was 1:50.4 for the synthesis of $PGMA_x$ (x≈50), 1:110.5 for the synthesis of $PGMA_x$ (x≈100). The number average x was calculated to be 50 and 100 by ^{1}H NMR based on integral ratios of resonance peaks from comparing the peak area of the initiator's -OCH_3 group at δ 3.35 ppm with that of the epoxide CH protons 3.21 ppm, and these numbers compared well with the targeted repeat unit numbers and the high GMA conversions. These samples were also analyzed by size exclusion chromatography (SEC) using DMF as the eluant. The polydispersity indices Mw/Mn were low at 1.19 and 1.22 for the two polymers based on PS calibration standards, and shown in Table 1.

The azide groups were introduced by reacting the oxirane rings of GMA with sodium azide. Matyjaszewski and coworkers confirmed that the azide anion attacked exclusively the less substituted carbon atom of the epoxide rings.[7,8] The completion of this reaction was confirmed by ^{1}H NMR and FT-IR. The signals of the CH and CH_2 protons of the epoxide ring at 2.62, 2.82, and 3.21 ppm disappeared in the P(GMA-N_3) spectrum after the reaction between PGMA and NaN_3. Moreover, this results was also accompanied by the disappearance of a characteristic FT-IR absorption peak at 909 cm^{-1} for the epoxide ring and the appearance of characteristic absorption peaks at 2104 cm^{-1} for the azide group and at 3500 cm^{-1} for hydroxyl group which shown in Fig. 2. The P(GMA-N_3) samples were also analyzed by SEC using THF as the eluant. Compared with their precursory PGMA, the apparent molecular weights of P(GMA-N_3) increased, and the polydispersity indices increased slightly as well.

PHFBMA-C≡CH and POEGMA-C≡CH. According to Scheme 2, PHFBMA-C≡CH and POEGMA-C≡CH were synthesized in two steps. First, reacting propargyl alcohol with 2-bromoisobutyric bromide following literature procedures yielded propargyl bromoisobutyrate

297 (ABIB). The latter was then used to initiate HFBMA and MEO_2MA polymerization to yield
298 PHFBMA-C≡CH and POEGMA-C≡CH, separately.

299 HFBMA polymerization in cyclohexanone using ABIB as the initiator was firstly reported
300 in this paper. At the ratios of $[HFBMA]_0/[initiatoir]_0/[CuBr]_0/ [bpy]_0$ of 25/1/1/2, it was found
301 that the well-defined polymer in cyclohexanone was easily produced. The resultant PHEMA-
302 C≡CH was characterized by ^{1}H NMR, and shown in Fig. 1. On the basis of ^{1}H NMR result,
303 comparing the peak area of the initiator's methylene protons (C≡C-CH_2-) at 4.71 ppm with
304 those of the ethyl groups of the hydroxyethyl group of HFBMA at 3.88 ppm yielded a repeat
305 unit number (actual DP) of 23. POEGMA-C≡CH was also synthesized by the ATRP of
306 MEO_2MA monomer using MBIB as the initiator. On the basis of ^{1}H NMR result, by
307 calculating the ratio both the area of the chemical shift of 4.71-4.73 ppm of CHC-CH_2-O-for
308 ABIB and that of 3.34 ppm of CH_3-O- for POEGMA, the actual DP of OEGMA was 41.

309 Table 1 Preparation conditions and molecular characteristics of the precursory polymers

Sample[a]	$[M_0]/ [I_0]$[b]	Yield[c] (%)	NMR DP[d]	NMR *Mn*[e] (kg/mol)	SEC *Mn*[f] (kg/mol)	SEC *Mw*/*Mn*[f]
$PGMA_{50}$	50.4:1	98	50	7.2	8.7	1.19
$PGMA_{100}$	110.5:1	90	100	13.8	17.2	1.22
$P(GMA\text{-}N_3)_{50}$	-	91	51	8.6	12.7	1.27
$P(GMA\text{-}N_3)_{100}$	-	86	97	16.4	20.4	1.30
PHFBMA-C≡CH	25:1	89	23	5.6	6.1	1.20
POEGMA-C≡CH	50:1	82	41	8.0	8.9	1.08

310 *[a] PGMA, P(GMA-N_3)x, PHFBMA-C≡CH, and POEGMA-C≡CH were prepared through the*
311 *ATRP. [b] The molar feed ratio is denoted as $[M]/[I]_0/[CuBr]_0/[L]_0$. [c] Yield was evaluated by*
312 *the gravimetric method. [d] The DPs were evaluated via ^{1}H NMR. [e] Mn was evaluated via ^{1}H*
313 *NMR. [f] Mn and Mw/Mn were evaluated by SEC using DMF as the eluent and PS standards.*

Binary graft copolymers (BGCs). PGMA-g-(PHFBMA-r-POEGMA) was synthesized by coupling P(GMA-N_3) with PHFBMA-C≡CH, and POEGMA-C≡CH. BGCs were started by graft reaction of PHFBMA-C≡CH chains onto P(GMA-N_3)x for 24 h, then POEGMA-C≡CH was added and reacted for another 48 h, at last followed by another 24 h with an excess of propargyl alcohol was added to exhaust the residual azide groups. Three binary graft copolymers denoted as BGC_1, BGC_2 and BGC_3 were prepared by grafting PHFBMA-C≡CH, and POEGMA-C≡CH. While P(GMA-N_3)$_{50}$ was used as the backbone for BGC_1 and BGC_2, the backbone used for BGC_3 was P(GMA-N_3)$_{100}$. The recipes used to prepare the copolymers and the molecular characteristics are listed in Table 2.

Table 2. Preparation conditions and molecular characteristics of binary graft copolymers

Sample[a]	Feed molar ratio[a]	$M_{n,\,theory}$[b] (kg/mol)	$M_{n,\,SEC}$ (kg/mol)	SEC M_w/M_n
BGC_1	50:10.0:5.0	116.6	123.2	1.16
BGC_2	50:10.0:10.0	144.6	139.5	1.17
BGC_3	100:20.0:20.0	288.4	248.9	1.20

a[$-N_3$] :[POEGMA-C≡CH]:[PHFBMA-C≡CH]. *b*$Mn_{,theory} = Mn_{(P(GMA\text{-}N3))} + x \times n \times 5600 + y \times n \times 8000$.

BGCs were analyzed by SEC, FT-IR and ^{1}H NMR. Fig. 3 compared the SEC traces of the precursors exclude P(GMA), P(GMA-N_3)$_{50}$, PHFBMA-C≡CH, POEGMA-C≡CH and BGCs. An important result was shown that no SEC peaks for the precursors were observed for the BGC_1 and BGC_2 prepared using the recipes shown in Table 2. This was due to the low molar ratios used for the polymer alkyne to azide groups used during the reactions. The molar ratios used between PHFBMA-C≡CH, and POEGMA-C≡CH and the azide groups of P(GMA-N_3) was 30%-40%, therefore, almost all the PHFBMA-C≡CH and POEGMA-C≡CH were reacted absolutely with P(GMA-N_3)x.

The FT-IR spectra of BGCs are shown in Fig. 4(a). The azide peak at 2104 cm^{-1} totally disappeared, and compared with P(GMA-N_3)x, the intensity of the peak at 1680 cm^{-1} increased obviously. Moreover, the ^1H NMR spectrum of BGC_1 measured in DMSO is shown in Fig. 4(b), all the protons of the grafted PHFBMA and POEGMA chains were observed in the spectrum measured in DMSO. A quantitative comparison of the integrals at 4.01 and 5.92-6.02 ppm yielded a molar ratio of 6.7:2.1 for the POEGMA and PHFBMA repeat units, respectively. These values compared well with the expected values of 7.5:2.5. Another observation was the presence of the signals at 7.9 and 5.2 ppm for the protons of the triazole linkage in the spectrum measured in DMSO-d_6. These peaks provided direct evidence for the desired click chemistry.

Self-assembly behaviors of BGCs

The micelle was readily obtained here using the solvent displacement method. 10 mg of BGC_1 was dissolved in 1.0 mL THF; under vigorous stirring 10 ml deionized water was added slowly at a flow rate of 0.2 mL/min until the appearance of the solution with a characteristic bluish tinge. After the addition was completed, the dispersion was left stirring for another 24 h at room temperature, and THF was blown away by nitrogen. Aqueous solution with light bluish tinge was typically obtained; similar procedures were done to prepared solutions with different concentrations for BGC_2 and BGC_3. The prepared micelles remained stable when left unstirred for three months.

The self-assembly behaviors were analyzed by DLS, TEM, and AFM, and the results are shown in Fig. 5. As shown in Fig. 5(a), the micelle with Z-average diameter of 114.3 nm with PDI=0.22, suggested that the binary graft copolymer BGC_2 existed as polymeric aggregates in aqueous solution, which is driven by the strong hydrophobic-hydrophilic interactions in the inner core and outer shell. To examine visually the size and morphology of BGCs, the typical TEM image of BGC_2 is presented in Fig. 5(b).

Spherical micelles were found to be uniformly dispersed with the diameter of 20 nm-70 nm. These micelles constructed from BGC_2 showed black core surrounded with light corona, presenting a typical micellar characteristic, and it was also apparent that the bigger nanoparticles were aggregated and formed by the small particles. This result could also be confirmed from the AFM results. Fig. 5(c) and (d) shows the AFM images of the BGC_2 micelle. The quantitative analysis yielded the AFM diameters of 30±10 nm, and mostly round as revealed by AFM.

Preparation of the superhydrophobic cotton fabrics with BGCs

Fig. 6 shows typical photographs of water droplets placed on cotton fabrics which had been modified with BGC_2 (a) and original cotton fabrics (b) at 30 ^{o}C with a humidity of ≈ 45%. For original cotton fabrics (b), water droplet was absorbed within about 10 s-20 s by the uncoated cotton fabrics due to its remarkable hydrophilicity and capillary forces. While for cotton fabrics modified with BGC_2 (a), 2 μL water droplet exhibited CA of 153±2^{o}. Although the water droplet gradually decreased until the droplet disappeared within 60 min-70 min, the CA did not change obviously during its evaporation process. According to the following SEM and AFM results, cotton fabrics modified with BGC_2 formed a thin protected layer, the capillary forces between cotton fibers and water droplet is negligible. Meanwhile, the thermodynamic stability of the modified cotton fabrics was also evaluated based on water droplet that remained on the modified cotton fabrics after the process of pressure imposing and releasing, and the result is shown in Fig. 7. The CA did not noticeably change after a pressure (≈0.1-0.3 kPa) was applied onto the droplet with modified cotton fabrics, thus these results indicated that superhydrophobic cotton fabrics were successfully prepared and exhibited long-term stability over times.

As described above, a superhydrophobic surface should have a rough structure as well as a chemical composition that provides a low surface free energy. In order to confirm the

chemical composition of the cotton fabrics coated with and absence of BGCs, the surface chemical compositions of the original and modified cotton fabrics were analyzed by ATR-FT-IR and XPS. Fig. 8 shows the FT-IR spectra of BGC_2, and ATR-FT-IR spectra of the cotton fabrics before and after coated with BGC_2. As shown in FT-IR spectrum of the BGC_2, signals appearing in this spectrum were consistent with the anticipated structure of this copolymer. The peak at 1740 cm^{-1} corresponded to carbonyl group absorption. Meanwhile, two broadened absorption peaks centered at 1285 cm^{-1} and 1160 cm^{-1} corresponded to $-CF_3$ stretching vibration absorptions. The asymmetrical C-O-C stretching vibration band was observed at 1060 cm^{-1}-1110 cm^{-1}, while two peaks at 705 cm^{-1} and 760 cm^{-1} could be attributed to a combination of C-F rocking and wagging vibrational absorptions. In the ATR-FT-IR spectrum of the original cotton fabrics, the peaks observed at 1060 cm^{-1}-1110 cm^{-1} were attributed to the C-O-C stretching vibration. In the ATR-FT-IR spectrum of the cotton fabrics modified with BGC_2, new absorption peaks appeared at 1285 cm^{-1} and 1160 cm^{-1}, which was consistent with the $-CF_3$ stretching vibration. Moreover, the intensity of the signals at 3340 cm^{-1} and 1060 cm^{-1}-1110 cm^{-1} had clearly increased over that of the uncoated cotton fabrics, and these signals corresponded to the stretching vibration bands exhibited by the O-H groups C-O-C chains of the copolymers, respectively. These results confirmed that the diblock copolymers were successfully coated onto the cotton fabrics. Fig. 9 shows the XPS spectra of the original cotton fabrics and cotton fabrics coated with BGC_2. While the surface of the uncoated cotton fabrics was dominated by C_{1s} and O_{1s} signals, a new F_{1s} signal was observed on the surface of the cotton fabrics coated with BGC_2, along with the C_{1s} and O_{1s} signals. This further demonstrated that the BGCs were successfully incorporated onto the surface of the cotton fibers.

It is believed that the cotton fabrics modified with BGCs not only had a low surface energy that was provided by the grafted PHFBMA chains, but also possessed enhanced roughness.

409 SEM and AFM measurements were employed to evaluate the surface roughness of the cotton
410 fabrics in and absence of BGC_2. As shown in Fig. 10(a), the woven structure of the cotton
411 fibers was visible in the SEM image of the original cotton fabrics at low magnification.
412 Moreover, many natural striations along the fiber and numerous gaps between the highly
413 intertwined fibers were observed in the SEM images that were recorded at higher
414 magnification in Fig. 10(b) and (c). These features indicated that the surface of the original
415 cotton fabrics exhibited a micro-scaled roughness. On the other hand, as shown in Fig. 10(d),
416 the woven microstructure of the fibers was also clearly visible in the SEM image of the
417 cotton fabrics modified with BGC_2 at low magnification, and the average diameter and the
418 numerous gaps between the highly intertwined fibers of the cotton fabrics did not change
419 after they had been coated with BGC_2. The similarity indicated that the inherent properties of
420 the cotton fabrics were retained.

421 In the SEM images recorded at medium magnification in Fig. 10(e), it appeared that the
422 fibers of the cotton fabrics modified with BGC_2 seemed to be smoother than those of the
423 unmodified cotton. However, the striations of the modified fiber were visible, and rough
424 structures were also visible on the surface of the cotton fabrics modified with BGC_2 in the
425 SEM image at high magnification, and shown in Fig. 10(f). These fine structures indicated
426 that the BGCs layer provided nanoscaled structural roughness on the surface of the fibers,
427 while the fibers themselves provided microscaled roughness at the surface of the cotton
428 fabrics modified with BGCs.

429 The surface roughness of the modified cotton fibers was further investigated by AFM
430 observation. Fig. 10(g) and (h) show the corresponding AFM topography images of the
431 original cotton fabrics and that coated with BGC_2, respectively. The original cotton fabrics
432 exhibited a relatively smooth surface with striations along the fibers, whereas nanoscaled
433 copolymer bumps with diameters ranging between 10 nm-30 nm were clearly discernible on

the surfaces of the fibers with BGC_2. This indicated that the nanoscaled roughness was successfully combined with the micro-scaled roughness on the fiber surface of the cotton fabrics. Such nano- and microscaled roughness was believed to contribute to the water-repellency of the cotton fabrics modified with BGCs.

Effect of copolymer structure on superhydrophobic property

The superhydrophobic cotton fabrics was achieved through the modification with BGCs, it was anticipated that the copolymer composition would affect the water repellency of the modified cotton fabrics. In order to study the water repellency of the cotton fabrics coated by BGCs with different compositions and various concentrations, the cotton fabrics were modified under the same conditions with the copolymers BGC_1, BGC_2, and BGC_3 at various concentrations.

The results of CAs and SAs of cotton fabrics coated with BGC_1, BGC_2, and BGC_3 at various concentrations are shown in Fig. 11(a) and (b). The results revealed that the relationship between the water repellency of the cotton fabrics modified with BGC_1, BGC_2, and BGC_3 at various concentrations behaved similar trends. The CAs increased dramatically to more than 150 ^{o} as the BGCs concentration was increased to 5 mg/mL, and then the increase of CAs slowed down and finally reached the plateau at 158^{o} when the concentration of BGC_1 was increased further to 10 mg/mL. Meanwhile, the SAs drastically decreased as the concentration of BGCs increased, and then leveled off at 4 ^{o}. Although the employed BGCs have different compositions and block lengths, the modified cotton fabrics eventually achieved very similar superhydrophobicity with CAs of 154^{o} and SAs of 7^{o}. These similarities suggested that the superhydrophobicity was mainly related to the quantities of the copolymers attached to the cotton fabrics, rather than the copolymer compositions and block lengths.

Reviewing the structure and composition of the copolymers listed in Table 2, However BGC_1, BGC_2, and BGC_3 had similar PGMA backbone, BGC_1 and BGC_2 had the same $PGMA_{50}$ backbone with varying PHFBMA contents, while the BGC_3 had longer $PGMA_{100}$ backbone but with the same PHFBMA content equal to BGC_2. For BGC_1 and BGC_2 with the same $PGMA_{50}$ backbone, the content of the PHFBMA block was ≈10 % for BGC_1, and ≈20 % for BGC_2, respectively. The minimum copolymer concentrations required to reach the same superhydrophobicity with CA of 150 ^{o} were 8.0 mg/mL for BGC_1, and 5.0 mg/mL for BGC_2, respectively. Furthermore, for BGC_3 with $PGMA_{100}$ backbone, the content of the PHFBMA block was also ≈20 %, to reach the same superhydrophobicity with CA of 150 ^{o} the minimum copolymer concentration was 5.0 mg/mL. The results indicated that less BGCs was required when the amount of HFBMA blocks was higher, and the more amount of HFBMA blocks, the higher the superhydrophobicity.

Here, the PHFBMA block was derived from the hexafluorobutyl methacrylate (HFBMA) monomer mainly due to its low surface free energy, HFBMA was inexpensive and environmentally friendly in comparison with other highly fluorinated monomers which are often used for fabricating superhydrophobic surfaces. Meanwhile, although the POEGMA block could not covalently adhere onto the surfaces of cotton fabrics, POEGMAs blocks have good compatibility with cotton fabrics, and they can be together well by intermolecular forces. Moreover, it was envisioned that the designed binary graft copolymers would self-assemble into micellar aggregates with PHFBMA blocks as the core and POEGMA block as the corona. Therefore, for cotton fabrics modification, hydrophilic POEGMAs segment interacts with cotton fibers and the hydrophobic PHFBMA segment migrates onto the fiber surface, and behaves superhydrophobic performance. The incorporation of these micellar nanostructures onto cotton fabrics could provide nanoscale roughness, which would combine with the microscale roughness inherent to the cotton fabrics with hierarchical roughness. The

schematic illustrations of the self-assembly of BGCs and mechanism for the generation of nano- and microscale structural roughness on the cotton fabrics have been illustrated in Scheme 3. The cotton fabrics modified process with BGCs was mainly carried out in aqueous media, and almost no organic solvents were involved, therefore, Therefore, the self-assembly method is first introduced to fabricate hydrophobic cotton fabrics. BGCs can self-assemble and produce stable water soluble PHFBMA-centered nano-micelles; then BGCs are used to fabricate hydrophobic cotton fabrics. While the PHFBMA block provides low surface free energy, the POEGMA block serves as an anchor with cotton fibers, the modified cotton fabrics show excellent superhydrophobic property. Considering all these factors such as severe conditions, tedious fabrications, and expensive materials limitations, the preparation of cotton fabrics with excellent superhydrophobic property proposed in this paper might has potential application prospect.

Durability of the cotton fabrics coated with BGCs

The durability of superhydrophobic surfaces is a very key consideration especially for practical applications. In this paper, the designed functional BGCs coated onto the cotton fabrics surface behaved excellent superhydrophobic properties, and it was also expected to behave durability. Therefore, the durability of cotton fabrics coated with BGCs was evaluated based on the variations of their water repellencies when exposed to different conditions over times. As shown in Fig. 11(c) and (d), the CAs decreased and their SAs increased after the modified cotton fabrics were immersed in various organic solvents, including ethanol, acetone, THF, and DMF, and in acidic or basic aqueous solutions for 72 h. It was found that the modified cotton fabrics showed better resistance against acidic or alkaline aqueous media, but behaved slightly weaker resistance against strongly organic environments. For example, the CAs decreased from 153^{o} to 120^{o} and the SAs increased from 5^{o} to 18^{o} when the modified cotton fabric was immersed in organic DMF, which might due to the gradual loss of

the attached BGCs by partial dissolution under organic solvents. While for modified cotton fabric immersed in the basic solution (pH≈ 12) for 72 h, the CAs decreased from 153° to 142° and the SAs increased from 5° to 11°. This might due to the gradual loss of the attached BGCs by partial hydrolysis of the ester groups under strongly alkaline conditions.[52,67] Although these cotton fabrics coated with BGCs showed relatively decreases of the CAs and SAs, these modified cotton fabrics also behaved some highly stable against chemical corrosion.

The mechanical stability of the modified cotton fabrics were also evaluated by abrading cotton fabrics modified with BGCs back and forth with sandpaper at a rate of about 5 cm s^{-1} under 1000g of force for repeated cycles, The results showed that both the CAs and SAs were decreased, the CAs decreased from 153° to 140° and the SAs increased from 5° to 9° for 20 repeated cycles, and the CAs decreased to 121° and the SAs increased to 20 ° for 50 repeated cycles. All of these results have demonstrated that the BGCs prepared by our current strategy were one of the good choices for the preparation of superhydrophobic cotton fabrics, and these superhydrophobic cotton fabrics might have many potential applications, such as self cleaning cotton textiles, waterproof yet air-breathable fabrics, swimwear, etc.

Conclusion

In summary, ATRP has been used to prepare PGMA, PHFBMA-C≡CH, and POEGMA-C≡CH, grafting PHFBMA-C≡CH, and POEGMA-C≡CH to P(GMA-N_3)x via click chemistry yielded functional binary graft copolymers, PGMA-g-(PHHFBMA-r-POEGMA) (BGCs), and these BGCs were used to fabricate superhydrophobic cotton fabrics. The self-assembly behaviors were investigated by combination of DLS, TEM and AFM, and the results indicated that BGCs self-assembled and produced stable water soluble PHFBMA-centered nano-micelles. Then BGCs micelles were used to fabricate superhydrophobic cotton fabrics. While the PHFBMA blocks provided the low surface free energy, the POEGMA blocks

served as anchors with the surfaces of cotton fibers, the modified cotton fabrics showed excellent water repellency with CA about 154^{o} and SA about 7^{o} under optimized conditions. The results confirmed that a fluorinated surface was formed onto a substrate without changing the bulk composition of the substrates. Moreover, nano- and microscale roughness were also created by combining BGC-based nano bumps onto surfaces of micro-sized cotton fabrics. As a result of tunability of hydrophobic and superhydrophobic properties, BGCs are of potential application prospects for the non-wetting surfaces fabrication.

Acknowledgements

The authors appreciate the Intergration of Industry, Education and Research of Guangdong Province project (project no. 2011A091000007), and Guangdong-Hongkong Technology Cooperation Finding (project no. 2009A091300012).

REFERENCES

1 Y. Y. Mai, A. Eisenberg, Chem. Soc. Rev. 2012, 41, 5969.

2 R. A. Ramli, W. A. Laftah, S. Hashim, RSC Adv. 2013, 3, 15543.

3 Y. F. Zhang, Q. Yin, H. Lu, H. W. Xia, Y. Lin, J. J. Cheng, ACS Macro Lett. 2013, 2, 809.

4 J. Jin, D. X. Wu, P. C. Sun, L. Liu, H. Y. Zhao, Macromolecules 2011, 44, 2016.

5 Z. P. Cheng, X. L. Zhu, E. T. Kang, K. G. Neoh, Langmuir 2005, 21, 7180.

6 B. W. Liu, H. Zhou, S. T. Zhou, H. J. Zhang, A. C. Feng, C. M. Jian, J. Hu, W. P. Gao, J. Y. Yuan, Macromolecules 2014, 47, 2938.

7 S. S. Sheiko, B. S. Sumerlin, K. Matyjaszewski, Prog. Polym. Sci. 2008, 33, 759.

8 N. V. Tsarevsky, S. A. Bencherif, and K. Matyjaszewski, Macromolecules 2007, 40, 4439.

9 Y. W. Li, H. L. Guo, J. Zheng, J. Q. Gan, Y. Zhang, X. X. Guan, K. Wu, M. G. Lu, RSC Adv. 2014,4, 54268.

10 A. Nese, J. Mosnacek, A. Juhari, J. A. Yoon, K. Koynov, T. Kowalewski, K. Matyjaszewski, Macromolecules 2010, 43, 1227.

11 F. Liu, J. W. Hu, G. J. Liu, C. M. Hou, S. D. Lin, H. L. Zou, G. W. Zhang, J. P. Sun, H. S. Luo, Y. Y. Tu, Macromolecules 2013, 46, 2646.

12 S. Chantasirichot, Y. Inoue, K. Ishihara, Macromolecules 2014, 47, 3128.

13 D. A. Z. Wever, F. Picchioni, A. A. Broekhuis, Ind. Eng. Chem. Res. 2013, 52, 16352.

14 C. L. Lo, C. K. Huang, K. M. Lin, G. H. Hsiue, Biomaterials 2007, 28, 1225.

15 A. Heise, J. L. Hedrick, C. W. Frank, R. D. Miller, J. Am. Chem. Soc.1999, 121, 8647.

16 H. Bellanger, T. Darmanin, E. T. Givenchy, F. Guittard, Chem. Rev. 2014, 114, 2694.

17 S. S. Latthe, C. Terashima, K. Nakata, A. Fujishima, Molecules 2014, 19, 4256.

18 B. Bhushan, Y. C. Jung, Prog. Mater. Sci. 2011, 56, 1.

19 Y. L. Zhang, H. Xia, E. Y. Kim and H. B. Sun, Soft Matter, 2012, 8, 11217.

20 S. S. Latthe, A. B. Gurav, C. S. Maruti, R. S. Vhatkar, Journal of Surface Engineered Materials and Advanced Technology 2012, 2, 76.

21 Z. G. Guo, W. M. Liu, B. L. Su, J. Colloid. Interface Sci. 2011, 353, 335.

22 J. Genzer, K. Efimenko, Biofouling 2006, 22, 339.

23 X. Zhang, F. Shi, J. Niu, Y. G. Jiang, Z. Q. Wang, J. Mater. Chem. 2008, 18, 621.

24 X. K. Liu, B. Y. Dai, L. Zhou, J. Q. Sun, J. Mater. Chem. 2009, 19, 497.

25 O. U. Nimittrakoolchai, S. Supothina, J. Eur. Ceram. Soc. 2008, 28, 947.

26 W. L. Song, A. C. Lima, J. F. Mano, Soft Matter 2010, 6, 5868.

27 E. K. Her, T. J. Ko, K. R. Lee, K. H. Oh, M. W. Moon, Nanoscale 2012, 4, 2900.

28 R. Almeida, J. W. Kwon, Langmuir 2013, 29, 994.

29 D. Xiong, G. J. Liu and L. Z. Hong, Chem. Mater. 2011, 23, 4357.

30 X. Deng, L. Mammen, H. J. Butt, D. Vollmer, Science 2012, 335, 67.

31 S. Y. Huang, ACS Appl. Mater. Interfaces 2014, 6, 17144.

32 K. S. Liu, X. Yao, L. Jiang, Chem. Soc. Rev. 2010, 39, 3240.

582 33 H. Zhou, H. X. Wang, H. T. Niu, A. Gestos, X. G. Wang, T. Lin, Adv. Mater. 2012, 24,
583 2409.
584 34 Q. Xie, J. Xu, L. Feng, L. Jiang, W. Tang, X. Luo and C. C. Han, Adv. Mater. 2004, 16,
585 302.
586 35 S. Ghiassian, H. Ismaili, B. D. W. Lubbock, Jo. W. Dube, P. J. Ragogna, M. S. Workentin,
587 Langmuir 2012, 28, 12326.
588 36 H. J. Butt, C. Semprebon, P. Papadopoulos, D. Vollmer, M. Brinkmann, M. Ciccotti, Soft
589 Matter 2013, 9, 418.
590 37 D. Xiong, G. J. Liu, E. J. S. Duncan, ACS Appl. Mater. Interfaces 2012, 4, 2445-2454.
591 38 T. Wang, X. G. Hu, S. J. Dong, Chem. Commun. 2007, 1849.
592 39 S. H. Park, S. M. Lee, H. S. Lim, J. T. Han, D. R. Lee, H. S. Shin, Y. J. Jeong, J. Kim, J.
593 H. Cho, ACS Appl. Mater. Interfaces 2010, 2, 658.
594 40 Z. K. He, M. Ma, X. R. Lan, F. Chen, K. Wang, H. Deng, Q. Zhang, Q. Fu, Soft Matter
595 2011, 7, 6435.
596 41 B. J. Basu, V. D. Kumar, C. Anandan, Appl. Surf. Sci. 2012, 261, 807.
597 42 D. Xiong, G. J. Liu, Langmuir 2012, 28, 6911.
598 43 M. L. Ma, M. Gupta, Z. Li, L. Zhai, K. K. Gleason, R. E. Cohen, M. F. Rubner, G. C.
599 Rutledge, Adv. Mater. 2007, 19, 255.
600 44 M. H. Jin, X. J. Feng, J. M. Xi, J. Zhai, K. Cho, L. Feng, L. Jiang, Macromol. Rapid
601 Commun. 2005, 26, 1805.
602 45 Z. G. Guoa, W. M. Liu, Plant Sci. 2007, 172, 1103.
603 46 H. Zhou, H. X. Wang, H. T. Niu, A. Gestos, T. Lin, Robust, Adv. Funct. Mater. 2013, 23,
604 1664.
605 47 F. P. Yi, R. T. Yu, S. X. Zheng, X. H. Li, Polymer 2011, 52, 5669.

606 48 J. Zimmermann, F. A. Reifler, G. Fortunato, L. C. Gerhardt, S. Seeger, Adv. Funct. Mater.
607 2008, 18, 3662.
608 49 H. Zhou, H. X. Wang, H. T. Niu, A. Gestos, X. G. Wang, T. Lin, Adv. Mater. 2012, 24,
609 2409.
610 50 Y. Wang, X. Y. Li, H. Hu, G. J. Liu, M. Rabnawaz, J. Mater. Chem. A 2014, 2, 8094.
611 51 Y. Zhao, Z. G. Xu, X. G. Wang, T. Lin, Langmuir 2012, 28, 6328.
612 52 H. L. Zou, S. D. Lin, Y. Y. Tu, G. J. Liu, J. W. Hu, F. Li, L. Miao, G. W. Zhang, H. S.
613 Luo, F. Liu, C. M. Hou, M. L. Hu, J. Mater. Chem. A 2013, 1, 11246.
614 53 M. Peng, J. Qi, Z. Zhou, Z. J. Liao, Z. M. Zhu, and H. L. Guo, Langmuir 2010, 26, 13062.
615 54 M. L. Ma, M. Gupta, Z. Li, L. Zhai, K. K. Gleason, R. E. Cohen, M. F. Rubner, G. C.
616 Rutledge, Adv. Mater. 2007, 19, 255.
617 55 L. Lin, M. J. Liu, L. Chen, P. P. Chen, J. Ma, D. Han, L. Jiang, Adv. Mater. 2010, 22,
618 4826.
619 56 B. Akhavan, K. Jarvis, P. Majewski, ACS Appl. Mater. Interfaces 2013, 5, 8563.
620 57 V. A. Ganesh, S. S. Dinachali, H. K. Raut, T. M. Walsh, A. S. Nair, S. Ramakrishna, RSC
621 Adv. 2013, 3, 3819.
622 58 P. F. Caamero, J. L. Fuente, E. L. Madruga, M. Fernandez-Garcia, Macromol. Chem. Phys.
623 2004, 205, 2221.
624 59 J. P. Sun, J. W. Hu, G. J. Liu, D. S. Xiao, G. P. He, R. F. Lu, J. Polym. Sci. Part A: Polym.
625 Chem. 2011, 49, 1282.
626 60 X. Deng, L. Mammen, Y. F. Zhao, P. Lellig, K. Müllen, C. Li, H. J. Butt, D. Vollme, Adv.
627 Mater. 2011, 23, 2962.
628 61 H. Bellanger, T. Darmanin, F. Guittard, Langmuir 2012, 28, 186.
629 62 G. P. He, J. W. Hu, G. J. Liu, Y. H. Li, G. W. Zhang, F. Liu, J. P. Sun, H. L. Zou, Y. Y.
630 Tu, D. S. Xiao, ACS Appl. Mater. Interfaces 2013, 5, 2378.

631 63 B. Wang, Y. B. Zhang, L. Shi, J. Li, Z. G. Guo, J. Mater. Chem. 2012, 22, 20112.

632 64 B. J. Shieh, F. J. Hou, Y. C. Chen, H. M. Chen, S. P. Yang, C. C. Cheng, H. L. Chen, Adv.

633 Mater. 2010, 22,597.

634 65 H. Teisala, M. Tuominen, M. Aromaa, M. Stepien, J. M. Mäkelä, J. J. Saarinen, M.

635 Toivakka, J. Kuusipalo, Langmuir 2012, 28, 3138.

636 66 G. W. Zhang, S. D. Lin, I. Wyman, H. L. Zou, J. W. Hu, G. J. Liu, J. D. Wang, F. Li, F.

637 Liu, M. L. Hu, ACS Appl. Mater. Interfaces 2013, 5, 13466.

638 67 G. Li, H. T. Zheng, Y. X. Wang, H. Wang, Q. B. Dong, R. K. Bai, Polymer 2010, 51,

639 1940.

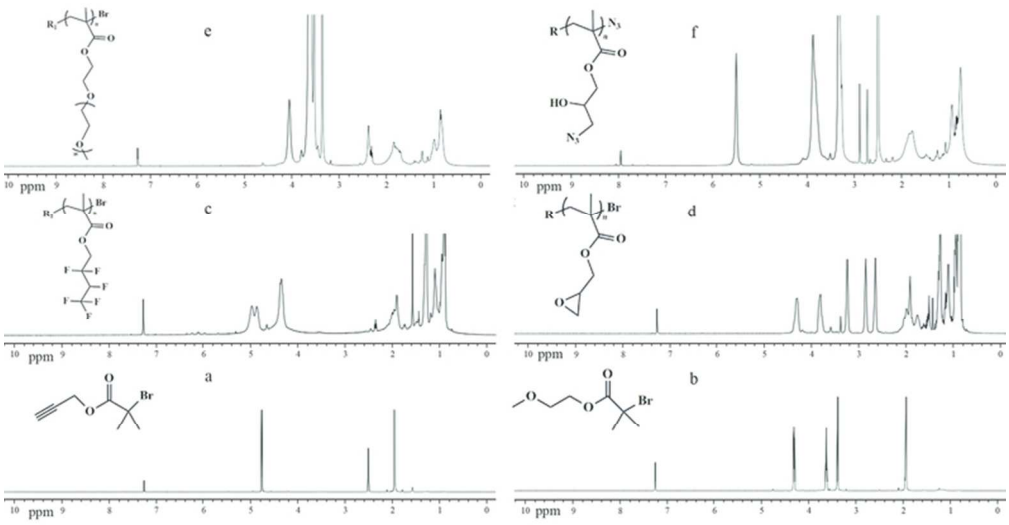

Fig. 1. The 1H NMR spectra of MBIB, ABIB, PHFBMA-C≡CH, PGMA50, POEGMA-C≡CH and (PGMA-N3)50.
67x35mm (300 x 300 DPI)

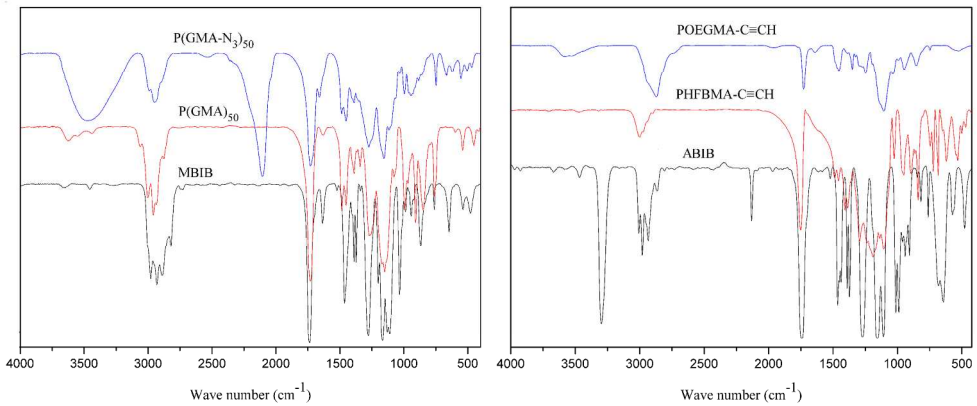

Fig. 2. The FT-IR spectra of ABIB, MBIB, PHFBMA-C≡CH, POEGMA-C≡CH, PGMA50, and (PGMA-N3)50.
241x105mm (300 x 300 DPI)

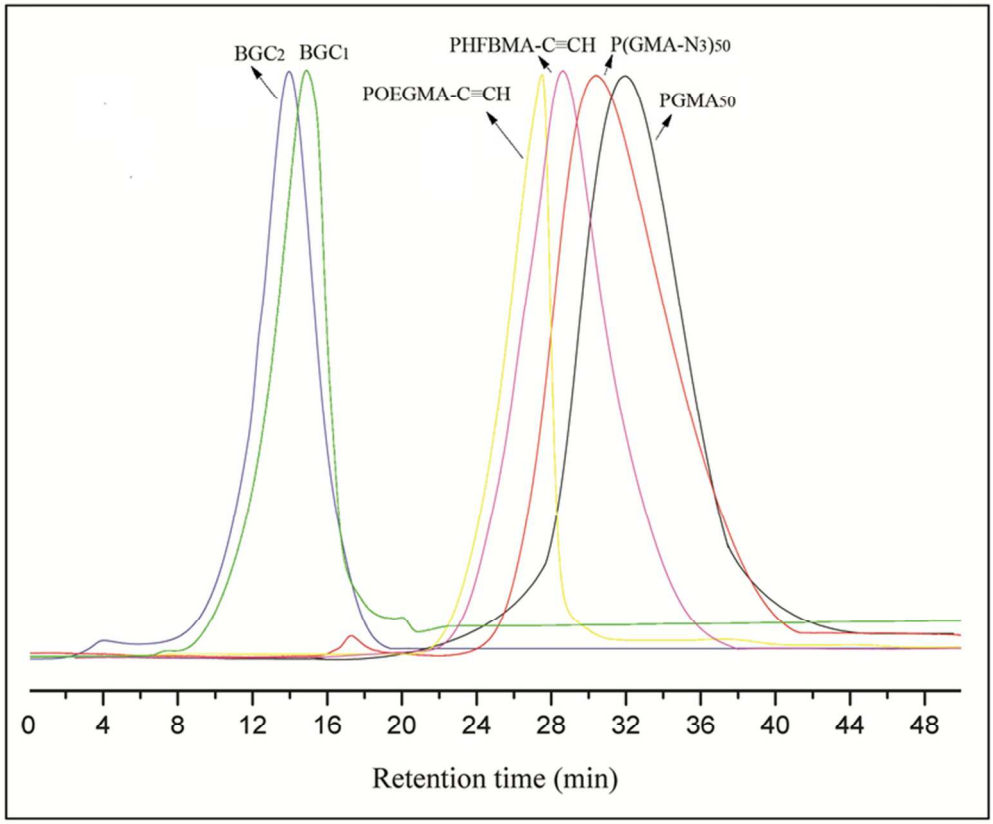

Fig. 3. SEC traces of polymer precursors and binary graft copolymers (BGCs).
71x59mm (300 x 300 DPI)

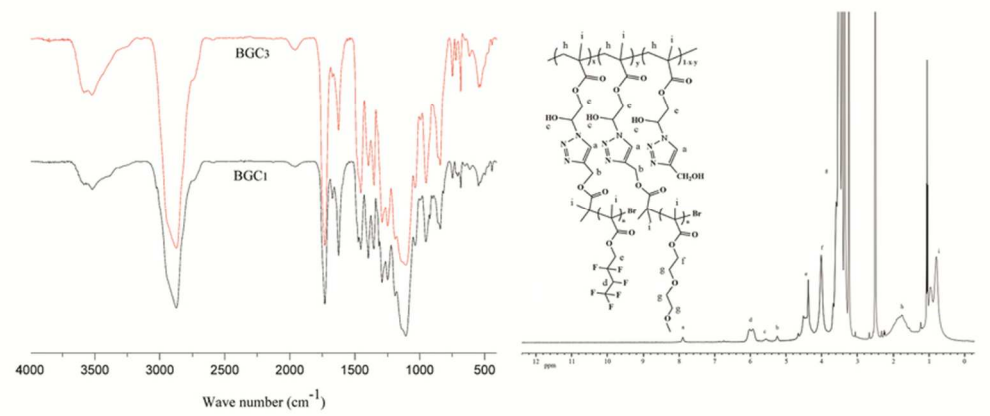

Fig. 4. The FT-IR spectra of BGC1 and BGC3, and 1H NMR spectrum for BGC2.
76x32mm (300 x 300 DPI)

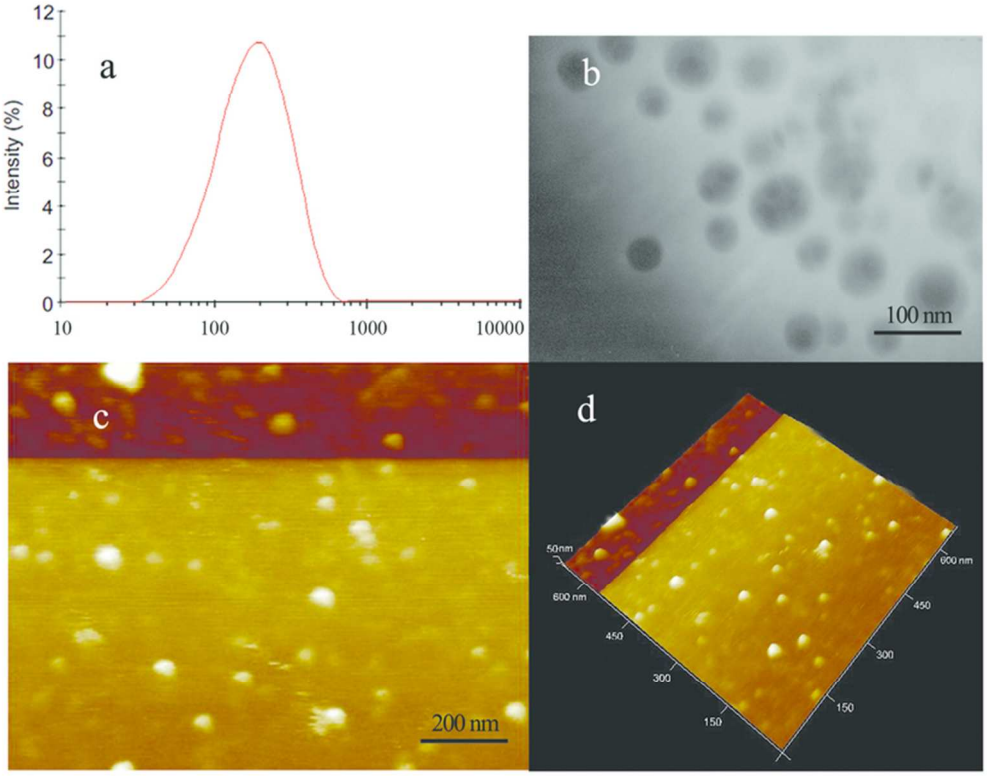

Fig. 5. The micellar particle size distribution (a) and morphology images (b, c and d) of BGC2.
70x55mm (300 x 300 DPI)

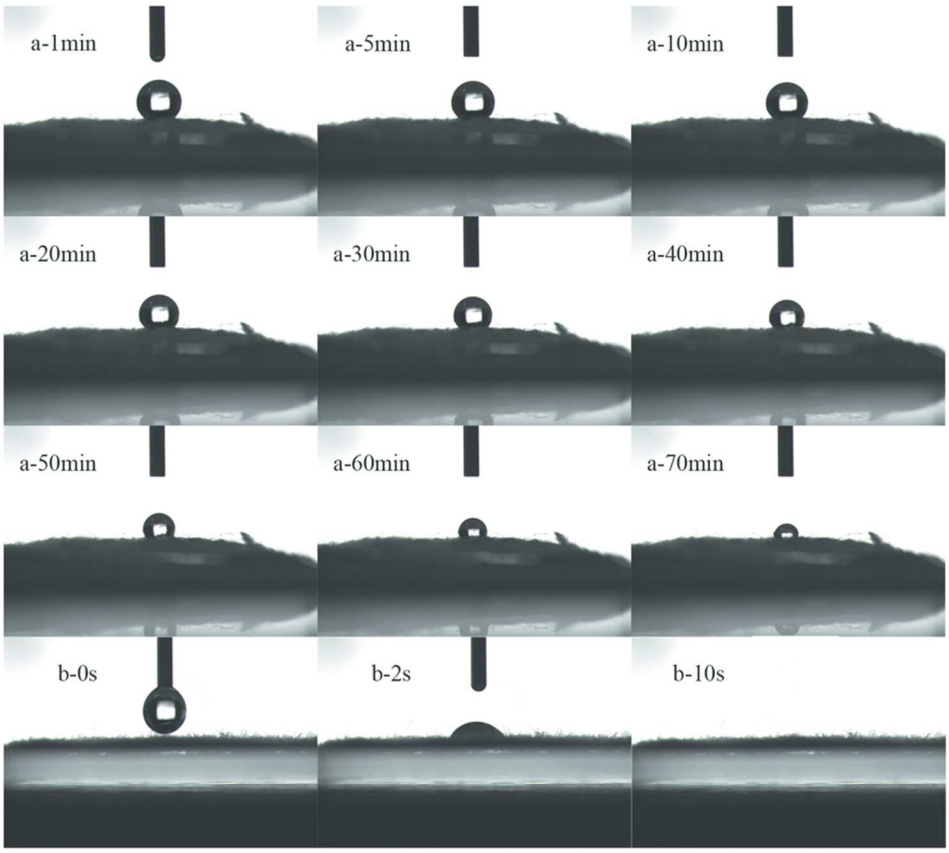

Fig. 6. Photographs of water droplet placed on cotton fabric modified with BGC2 (a) and on original cotton fabric (b).
81x73mm (300 x 300 DPI)

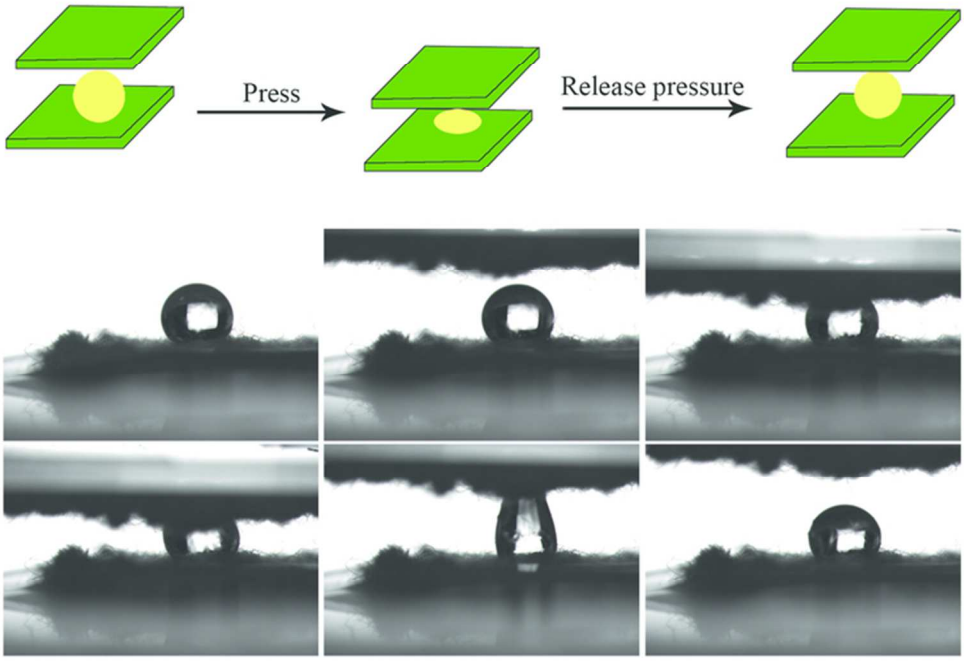

Fig. 7. Photographs of water droplet placed on cotton fabric modified with BGC2 as subjected to pressure imposing and releasing process.
64x46mm (300 x 300 DPI)

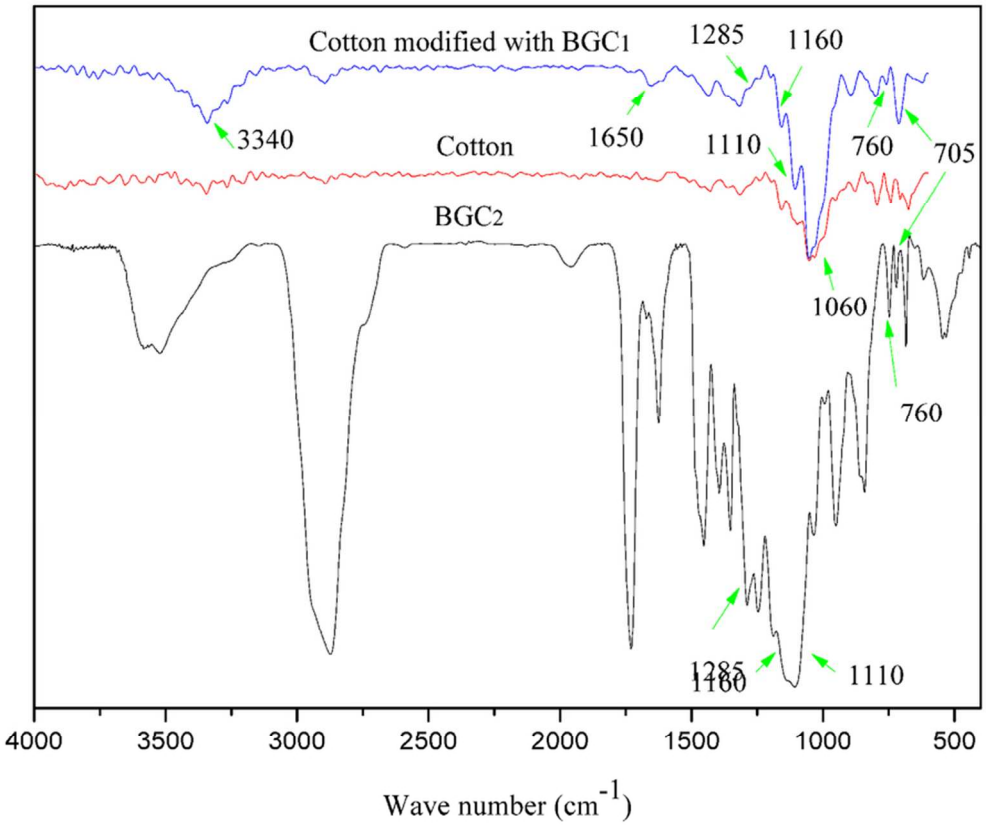

Fig. 8. FT-IR spectrum of BGC2 and the ATR-FT-IR spectra of the original cotton fabric and cotton fabric modified with BGC2.
76x65mm (300 x 300 DPI)

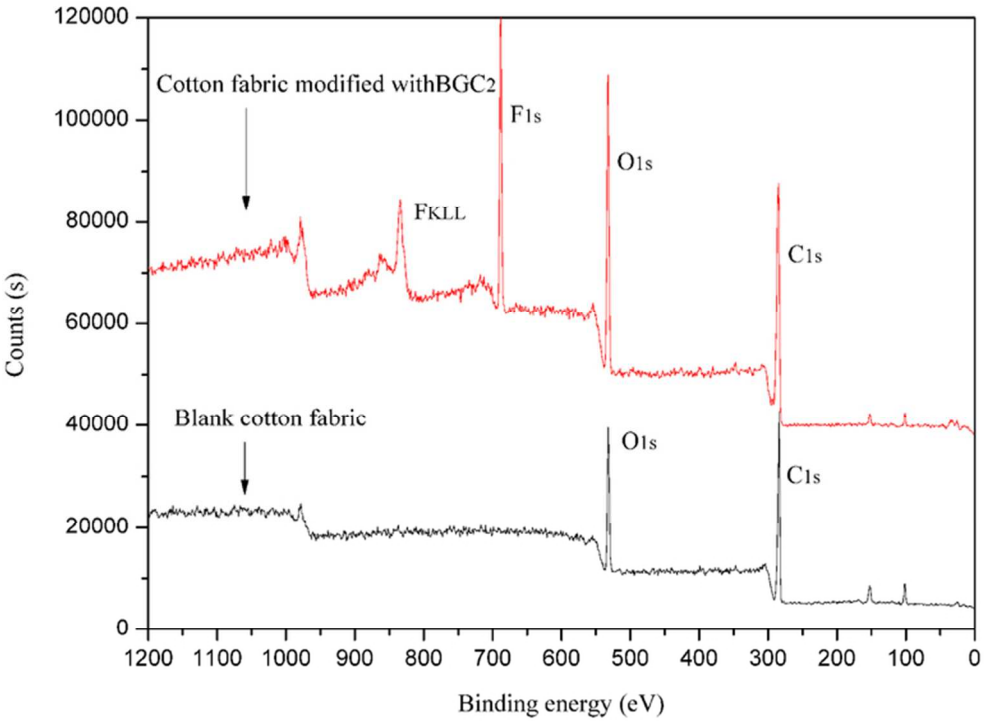

Fig. 9. XPS spectra of the original cotton fabric and cotton fabric modified with BGC2.
66x48mm (300 x 300 DPI)

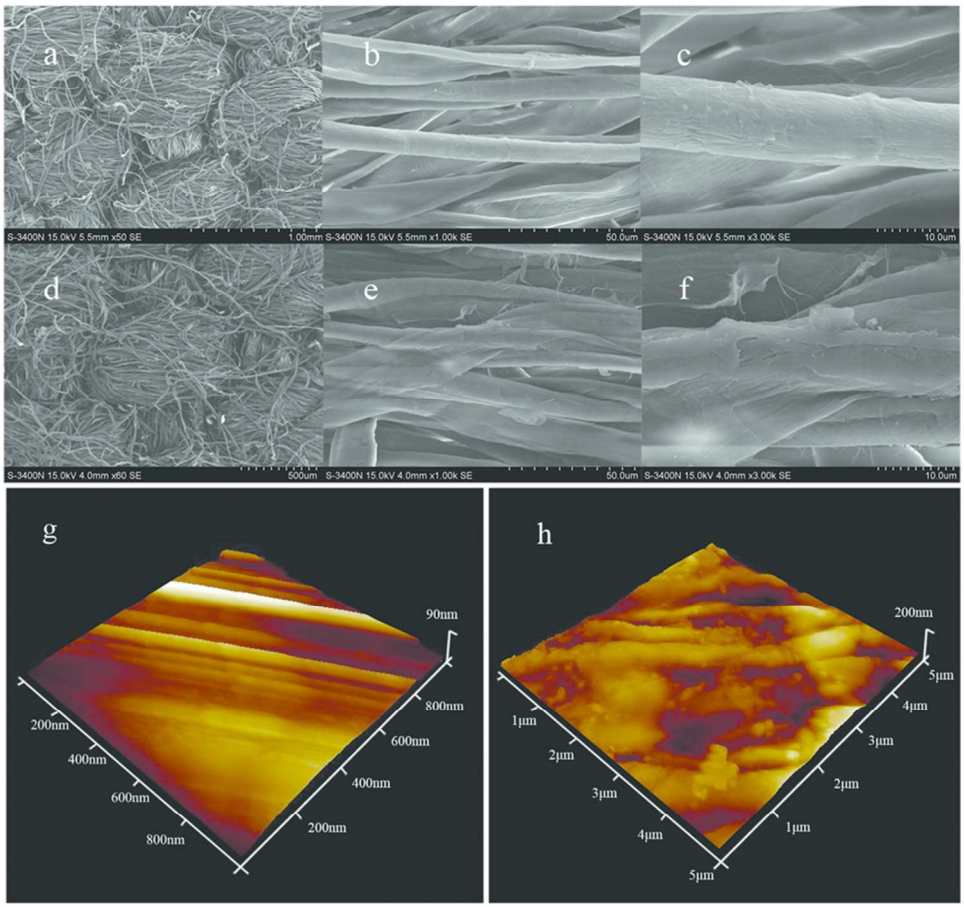

Fig. 10. SEM images and AFM topography images of the original cotton fabric (a, b, c, g) and cotton fabric modified with BGC2 (d, e, f, h).
76x71mm (300 x 300 DPI)

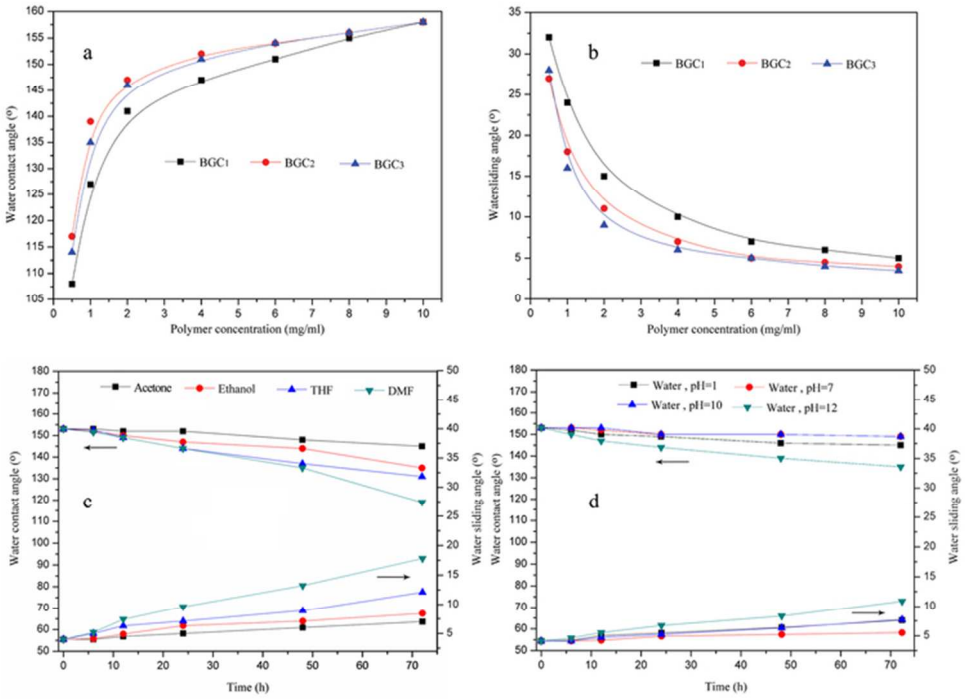

Fig. 11. Water repellency (a and b) of cotton fabrics modified with BGC1, BGC2, and BGC3 at various concentrations, and variation of water repellency of cotton fabrics modified with BGC2 with time: immersion in various organic solvents (c), immersion in aqueous solutions at different pH values (d).
65x48mm (300 x 300 DPI)

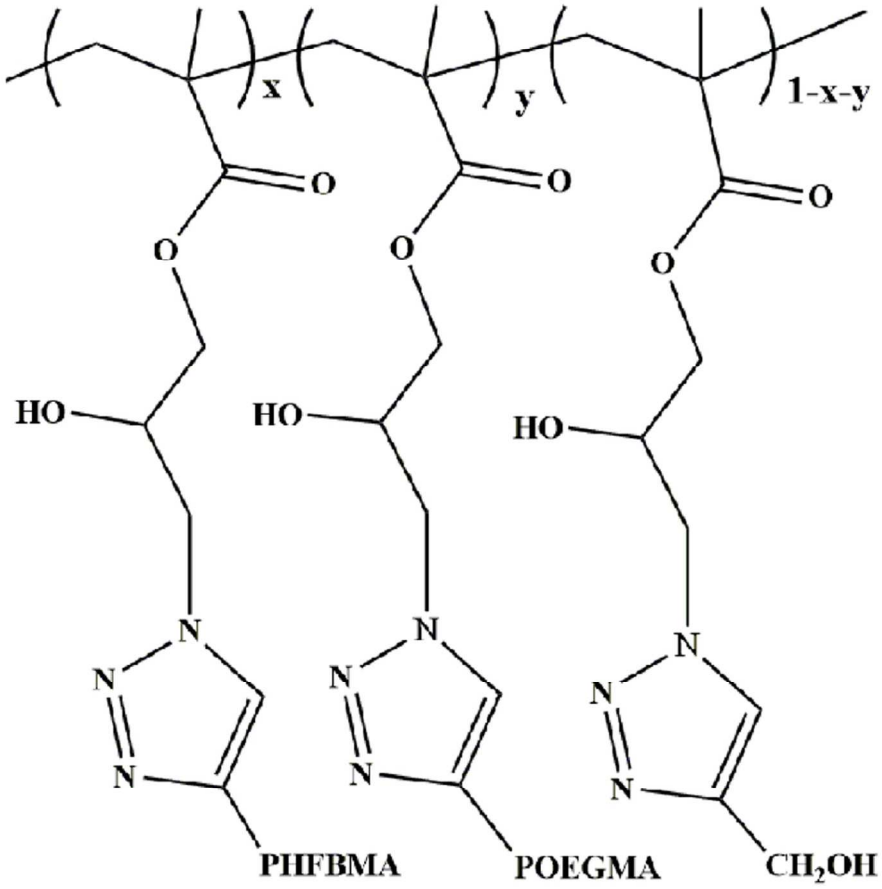

Scheme 1. Structure of PGMA-g-(PHFBMA-r-POEGMA).
85x81mm (300 x 300 DPI)

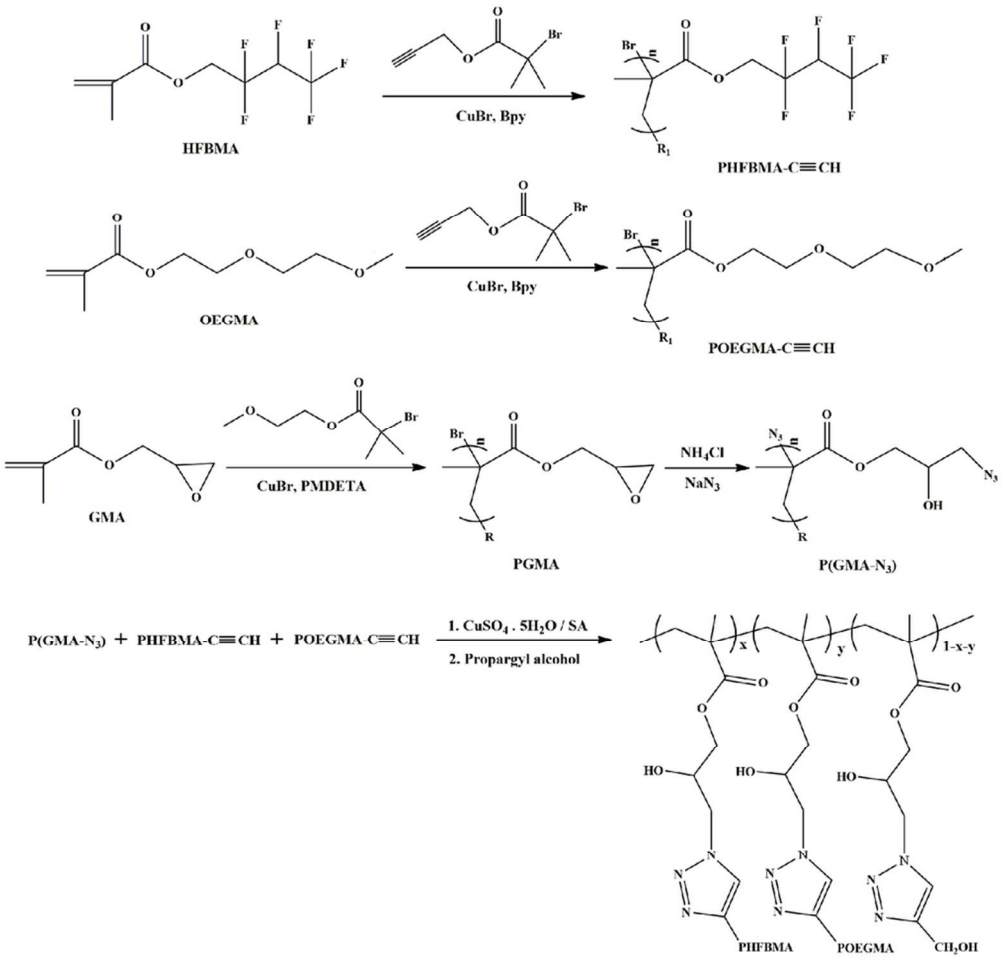

Scheme 2. Synthetic routes toward PGMA-g-(PHFBMA-r-POEGMA).
85x81mm (300 x 300 DPI)

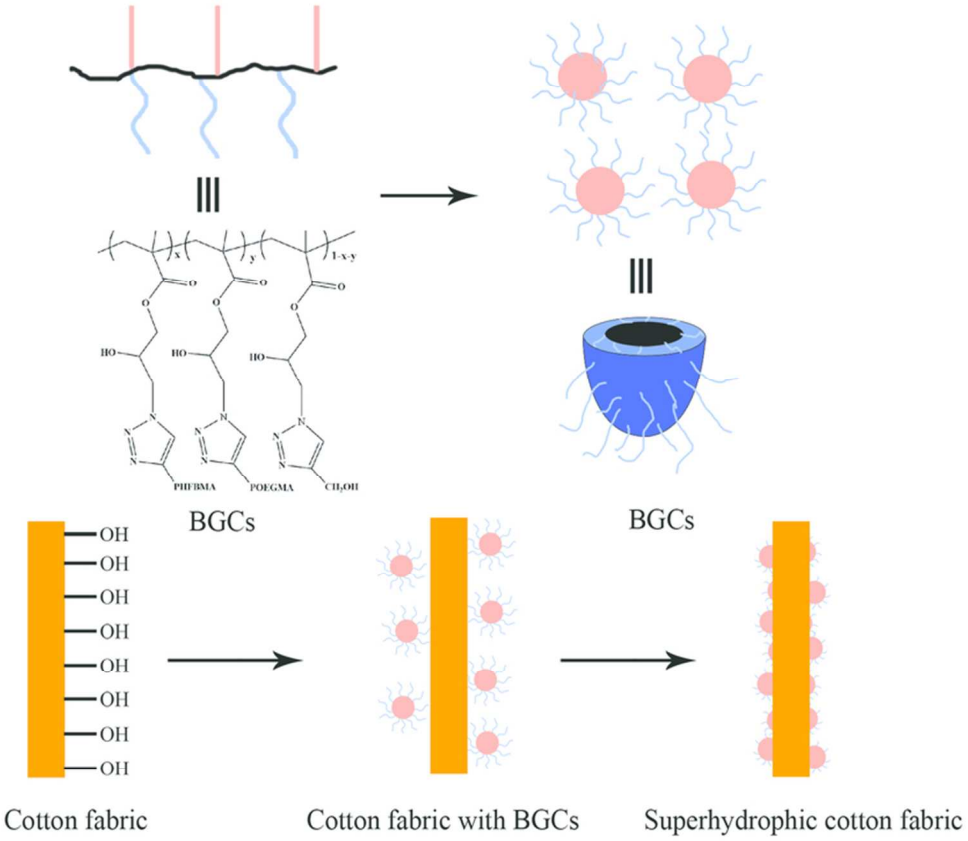

Scheme 3. Schematic illustrations of the self-assembly of BGCs and mechanism for the generation of nano- and microscale structural roughness on the cotton fabrics.
73x64mm (300 x 300 DPI)